

Apr 19th, 10:00 AM - 11:15 AM

Medical

Yuqing Liu
UNT

Nicole Hatch

Toluwani Ogunbayode

Siddhant Shelke

Corey Olszewski
UNT

Follow this and additional works at: <https://digitalcommons.collin.edu/ccuisrc>

Liu, Yuqing; Hatch, Nicole; Ogunbayode, Toluwani; Shelke, Siddhant; and Olszewski, Corey, "Medical" (2018). *Collin College Undergraduate Interdisciplinary Student Research Conference*. 9.
<https://digitalcommons.collin.edu/ccuisrc/2018/thursday/9>

This Panel is brought to you for free and open access by DigitalCommons@Collin. It has been accepted for inclusion in Collin College Undergraduate Interdisciplinary Student Research Conference by an authorized administrator of DigitalCommons@Collin. For more information, please contact mtomlin@collin.edu.

Investigating the Effects of Time-Mediated Addition of Titanium Dioxide Nanoparticles on the Differentiation and Proliferation of Human Dental Pulp Stem Cells

Abstract

Dental pulp stem cells (DPSCs) have therapeutic promise due to their rapid proliferation and multipotency but require further research to reach their full potential. Titanium dioxide nanoparticles (TiO₂ NPs) possess properties for cell tracking and imaging, but their harmful effects on cell viability and function pose roadblocks to their usage. This study investigates the timing of TiO₂ NP addition to DPSCs, a commonly neglected variable when testing NP toxicity, and its effects on DPSC proliferation and differentiation. Based on preliminary testing, DPSCs can respond to polybutadiene substrate mechanics after a 4-day incubation period. Accordingly, we added TiO₂ NPs on both days 1 and 4 (NP-1 and NP-4, respectively) after plating DPSCs on hard polybutadiene films. Through the lens of mechanical properties, this study explores the influence of time-mediated TiO₂ NP addition and examines its effects on DPSC viability, proliferation, and differentiation before and after recognition of polybutadiene-coated substrate. Results showed that NP-4 had substantially reduced harm to DPSC proliferation and differentiation as compared to NP-1, suggesting that time-mediated addition can prevent adverse effects of TiO₂ and NPs as a whole. These results can be translated to many other applications including drug delivery, developmental biology, biosensing, and biological imaging.

I. Introduction

(I. A.) Background Information

Stem cells have gained attention from scientists, medical professionals, and the general public for their possible applications in the emerging fields of tissue engineering and regenerative medicine.¹ As undifferentiated cells with the distinct ability to self-renew indefinitely and differentiate into various types of specialized cells, stem cells offer new avenues in the treatment of diseases using cell-based therapies.² Research regarding stem cells continues to expand due to their tremendous potential in revolutionizing medical care.³

While stem cells can originate from all over the body—for example, skin, bone marrow, and muscle tissues—human dental pulp stem cells (DPSCs) specifically have been widely studied due to their rapid proliferation rates, easy accessibility, multipotent differentiation, and less invasive harvesting compared to stem cells taken from bone marrow.⁴ In addition, DPSCs can be easily cryopreserved and revived, allowing for more flexibility for future usage in laboratories and therapies.⁵ Moreover, DPSCs can differentiate into a variety of cell lines, including osteoblasts, odontoblasts, and chondrocytes, allowing them to regenerate and repair many different types of damaged tissue.⁶ Because of this, DPSCs are currently being tested to treat a variety of conditions including type 1 diabetes, neurological diseases, immunological diseases, and diseases of the bone and cartilage.⁷ Despite this progress, further imaging and characterization of stem cell properties and functions are needed for DPSCs to reach their full therapeutic potential.⁸ Controlling and monitoring DPSCs *in vitro* for applications *in vivo* requires non-invasive mechanisms to track and image cells.

This goal can be addressed with nanotechnology, as nanoparticles (NPs) provide solutions and other benefits when added to and inside of cells. Among the most popular of these particles is (rutile) titanium dioxide (TiO_2), a well-known and low-cost material, with ideal properties such as semiconductivity.⁹ Commercially, TiO_2 NPs are used in sunscreens, lotions, toothpastes, and various cosmetics due to their strong catalytic activity.¹⁰ In dentistry, TiO_2 is used in dental composites and root canal surgeries for their strong antimicrobial properties, biocompatibility, and higher stiffness.¹¹ TiO_2 NPs thus possess a wide range of applications when used to enhance or observe cellular development.

However, despite their substantial promise, TiO_2 NPs have been found to be potentially harmful to cells. Contrary to a conventional characterization of TiO_2 as a “white knight” with low toxicity and chemical inertness,¹² recent studies have shown various adverse effects as a result of TiO_2 exposure. For example, TiO_2 NPs have been shown to decrease cell proliferation and impair the cellular functions of human dermal fibroblasts.¹³ Specifically regarding stem cells, uptake of TiO_2 NPs can negatively affect the proliferation, viability, and differentiation of bone marrow mesenchymal stem cells¹⁴ and inhibit short term DPSC proliferation at concentrations as low as 25 $\mu\text{g/mL}$.¹⁵ More broadly, TiO_2 NPs have also been seen to cause oxidative stress, carcinogenesis, genotoxicity, and immune disruption.¹⁵

(I. B.) Experimental Objective and Rationale

This study seeks to investigate the risk for using TiO_2 as in those products, as it is still an open question, but the focus of our experiment is the modulation of a never before considered variable in NP-cell interaction, which we hypothesized could potentially reduce or change the extent of harmful effects of TiO_2 in laboratory cellular work. In doing so, the applications of

using NPs and TiO₂ in particular can be recognized. When inside cells, TiO₂ NPs are able to regulate the release and kinetics of critical growth factors to improve *in vivo* conditions.¹⁶ For DPSCs, TiO₂ NPs can also be used as a non-invasive mechanism for greatly improving cell tracking¹⁷ and imaging¹⁸ due to their fluorescent properties and ability to penetrate cells. This allows scientists to examine the movement of the cells in a body or in an injected gel and is critical to the future of stem cell research and application. Additionally, TiO₂ NP's can play a role in developing targeted drug delivery technologies, as they not only serve as carriers and can release the drug,¹⁹ their tracking element ensures that the correct areas are receiving the drug. TiO₂ NPs thus possess the potential for a wide range of important and cutting-edge applications when used to enhance or observe cellular development, granted there can be a way to protect cellular health and viability.

Understanding the various factors affecting NP-cell interactions is paramount to minimizing the potentially negative effects of adding TiO₂ NPs. In all previous investigations and literature regarding NP-cell interactions, however, there has always been one neglected factor: the timing of the addition of NPs (they had always been added on the first day). We decided to introduce this variable and examine the effects of time-mediated NP insertion, which could provide a novel method to diminish the harmful effects of TiO₂ NPs. Previous work has suggested that, over time, cells can recognize the stiffness of their substrate and adjust their mechanical properties to match that of their substrate,²¹ and of course all cells develop and change over time as a culture grows. Furthermore, given that physical properties of cells have significant effects on biological function,²² especially stem cell maintenance and differentiation,²³ different cell mechanical properties before and after this “substrate recognition” could result in

different outcomes when nanoparticles are added on those days. The timing of this substrate recognition determined our time points for the addition of TiO₂ NPs, which preliminary testing showed to be on day4, and we chose to use a hard substrate, which would cause the cells to adjust to be mechanically stronger by that day.

Accordingly, we compared two experimental groups with rutile TiO₂ NPs added on day 1 of culturing (before cells responded to surface mechanics) and day 4 (after cells responded to surface mechanics) in addition to a control group without NPs. These cells were grown to differentiate into osteoblasts, and a comparison of the three groups of cells would allow us to determine the effects of TiO₂ NPs on DPSCs when added at the normal time and a later time. We considered differences in NP uptake mechanism and immediate effect, short term proliferation, and the different DPSCs' abilities for osteogenic differentiation after a longer period of time.

II. Materials and Methods

(II. A.) Cell Culture and Fixation

The first step was to create an environment for the cells, which was a 20 nanometer PB film (over a Si wafer) as a hard substrate, and alongside an Alpha MEM growth medium of 10% FBS, 200μM L-ascorbic acid 2-phosphate, and 10mM β-glycerophosphate is an environment for osteogenesis.²⁴ Our goal was not to control when or how differentiation occurred, but to test the cells could even do so after up to 21 days, so we used that working substrate and medium. We used cut wafers and wells of different sizes for different purposes, but spin coated a thin, hard layer of PB over each of them and cultured DPSCs to all of them on day 0 with the same cell solution. First, using a diamond cutter and tweezers, we cleaved silicon wafers needed for the substrates into the 1x1 and 2x2 cm squares, with the small samples for confocal microscopy and

SEM and the larger samples for AFM. Before we spin casted the cleaved wafers to coat them, they were put through a series of washes to prevent possible contamination and ensure optimal conditions for creating a hard, stiff polybutadiene (PB) film.²⁴ To do so, we performed separate processes to remove dust and organics before making the surface hydrophilic to preserve the cleaned wafers in water. The hardness of the substrate required a thin PB film, with thickness being determined by the concentration of the solution being spin casted. To create that solution, we measured 15 mg of PB out on an electronic scale and dissolved it into 5 mL of toluene to form a [3mg/mL] PB-toluene solution.

We spin casted the PB-toluene solution onto the prepared silicon wafers to create the 20 nm thick hard PB film. Because the PB-toluene solution was hydrophobic, we immersed the wafers in $\text{H}_2\text{O}:\text{HF} = 30:1$ immediately prior to spin casting until the surface became hydrophobic. We then pipetted PB-toluene solution onto wafers until the surface was fully covered. We spin casted the wafer at 2500 rpm at a 1000 ramp acceleration for 30 seconds. Finally, we annealed the spin casted samples in a high-powered vacuum oven set to 10^{-7} torr at 150°C for 12 hours to sterilize the wafer and flatten the PB film.

We then plated DPSCs (cell line AX3) onto prepared substrates on day 0, pipetting the cell solution onto substrates inside wells along with our aMEM medium. We plated approximately 7,500 and 15,000 cells on each small and large well, respectively. Based on previously calculated concentration of the cell solution (by counting a sample of the solution with a hemocytometer), this corresponded to 1 mL of medium needed for small 1x1 samples and 3 mL of medium for large 2x2 samples. After autoclaving, we then added sterilized rutile TiO_2 NPs to experimental groups NP-1 and NP-4 on days 1 and 4, respectively. To do so, we added 40

mL of medium to the 4 mg of TiO₂ NPs to create a 0.1 mg/mL solution. We aspirated the previous medium in the wells, and we pipetted 1 mL of the TiO₂-medium solution into each experimental well.

For each day of testing, cell fixation on every sample was performed for images under confocal microscopy and scanning electron microscopy (SEM), discussed later. To prevent contamination, the gloves and fume hood were sprayed with 70% ethanol. Sample wells were then aspirated until only the cells and substrates remained. 1 mL of sterilized PBS solution was then pipetted into each well and aspirated immediately afterwards. This aspiration procedure was done twice with PBS and then placed into 10% formalin for 15 minutes to kill cells while maintaining their shape and structure, completing the preservation process. After washing with PBS twice, the cells were preserved in a 4°C refrigerator for later use.

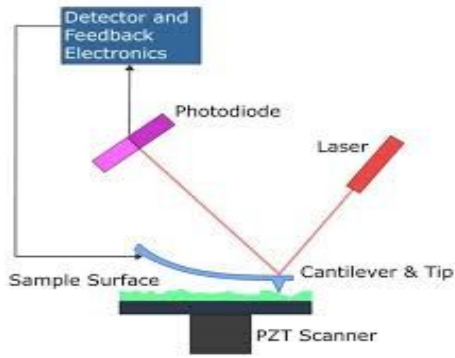


Fig. 1: Operation Principle of Contact Mode Atomic Force Microscopy (AFM)²⁵

(II. B.) Atomic Force Microscopy

To determine cell mechanical properties in relation to the substrate, we performed shear modulation force microscopy (SMFM) using a Digital Instruments Atomic Force Microscope (AFM) set to contact mode. As depicted in Figure 2, a tiny cantilever and tip make soft physical contact with the surface of the cells, dragged along at drive

amplitudes. Based on the cells' resistance to deformation and corresponding friction, the response amplitude is captured by the laser and photodiode, thus measuring cell stiffness. We plotted varying drive and subsequent response amplitudes for each SMFM measurement for a wider range of data.

We used a Bruker Dimension Icon with ScanAsyst to analyze the surface morphology of each spin-coated sample. They were then scanned in peak force tapping mode and analyzed using Bruker's NanoScope Analysis software. The data for this software would later be used to calculate the cells' shear modulus values, which will be explained later in results. Every test day, we first performed SMFM on a regular 20 nm PB film before testing to create a base calibration for later SMFM measurements of DPSC cells. After we calibrated the substrates, we placed samples under the AFM, and we performed testing twice for 3 chosen cells in each of two samples for a total of 6 measurements per experimental group.

(II. C.) Scanning Electron Microscopy

We characterized cross sectional images of DPSCs to view nanoparticle uptake in cells via focused ion-beam-scanning electron microscopy (FIB-SEM) using a LEO/Zeiss 1550 emission scanning electron microscope with a Zeiss Crossbeam 340 attachment at 1 kV acceleration voltage and 5 mm working distance. Cells were fixed in 2% glutaraldehyde/2% paraformaldehyde for 1 hour and stained using the OTOTO method²⁶ commonly used to increase the contrast of SEM images. We then used Acetone/DI water mixtures at gradually increasing concentrations from 30% to 100% to dehydrate samples before sputter coating with Au for 4 nm. After samples were prepared, We deposited Pd onto cells for protection from the focused ion beam. The FIB then milled the cell, exposing the cell cross section and allowing the SEM to take a series of cross-sectional stack images.

Furthermore, we captured the elemental composition of DPSCs using regular SEM equipped with Oxford energy dispersive X-ray spectroscopy (SEM/EDX) on day 21 in order to characterize biomineralization, or the cell-mediated process of depositing minerals into their

extracellular matrix. Images were taken at 10 kV acceleration voltage and 5 mm working distance. In preparation for SEM/EDX, we took samples from incubators and allowed them to rest for 1 day to naturally detach cells from the substrate. We then washed the substrates in distilled water and air-dried them for 1 day before having them sputter-coated with gold to create a 4 nm similar to the FIB-SEM.

(II. D.) Confocal Microscopy

To determine DPSC morphology, and count cells, we observed previously fixed cells preserved in PBS under a Leica Microsystems confocal microscope (Wetzlar, Germany). We tested days 1, 2, 4, 5, 8, and 21, with day 21 being for the purpose of viewing osteocalcin expression. For each day of testing, we performed cell fixation on every sample for images under confocal microscopy. To prevent contamination, we sprayed the gloves and fume hood with 70% ethanol. We then aspirated medium from the medium from the wells. We then pipetted 1 mL of sterilized PBS solution into each well and aspirated immediately afterwards. We conducted this aspiration procedure twice with PBS, and we then placed the sample into 10% formalin for 15 minutes to kill cells while fixing cells to preserve their structures. After washing with PBS twice, the cells were preserved in a 4°C refrigerator for later use.

Prior to using the microscope, we added dyes to samples to view certain parts of the cell. We stained actin and nuclei using Alexa Fluor 488 (AF488) and 4',6-diamidino-2-phenylindole (DAPI) dyes, respectively, in order to image specific aspects of cells. We washed cells in 0.4% Triton for 7.5 minutes to permeabilize cell membranes and allow dyes to enter. We then added AF488 for 20 minutes, followed by two washes of PBS. Next, we added a 5 µg /mL DAPI solution to cells for 3 minutes. We then washed cells twice more in PBS. In the day 21 samples,

we stained osteocalcin with osteocalcin antibodies (OCN). Given that osteocalcin gene expression is a marker of DPSC mature osteogenic and odontogenic differentiation and shows up by day 21,²⁷ we used osteocalcin levels as a measurement of DPSC differentiation. Before adding OCN, we added 0.1% BSA in PBS to the cells for 60 minutes to prevent OCN from non-specific and thus increase the chance that OCN binded to the target osteocalcin. We then added OCN to the cells for 2 hours at room temperature. Then we washed the samples 3 times in 0.1% BSA solution for 5 minutes each. We then repeated the previously described procedure for AF488 and DAPI staining, but we replaced washes in PBS following each step with washes in 0.1% BSA solution for 5 minutes.

The microscopy was done with a 405 nm diode and white light laser to excite the dyes. We took 5 images with 10x zoom at different times on different areas of each sample group and used ImageJ software²⁸ to manually count cells with sharpened contrast between the background and nuclei. Other images used 40x zoom; actin images were used as qualitative data to describe cell mechanics, and osteocalcin intensity data was calculated.

III. Results and Discussion

(III. A.) Mechanical Properties and NP Uptake

The first important results we obtained were regarding the uptake of the particles, and analysis of mechanical properties was important to attempt to explain it. Our consideration of mechanical properties included quantitative shear modulus data (higher is stronger) and qualitative microscopy images of actin. The former was calculated by graphing plotting drive amplitude vs. response amplitude for each SMFM measurement of the film calibration and

samples and using the average slope of these regression lines to calculate for the shear modulus of each day, given by the following formula:²⁹

$$\left(\frac{\overline{m}_{film}}{\overline{m}_{cell}} \right)^{1.51},$$

where \overline{m}_{film} represents the mean slope values of the film calibration and the cell value is the average of measurements for the cell samples. We performed SMFM and the calculation on samples on days of nanoparticle addition (1 and 4) and the days immediately after (2 and 5), while tracking the control at more points to show the trend of substrate recognition. These shear modulus values were then plotted to form the following graphs:

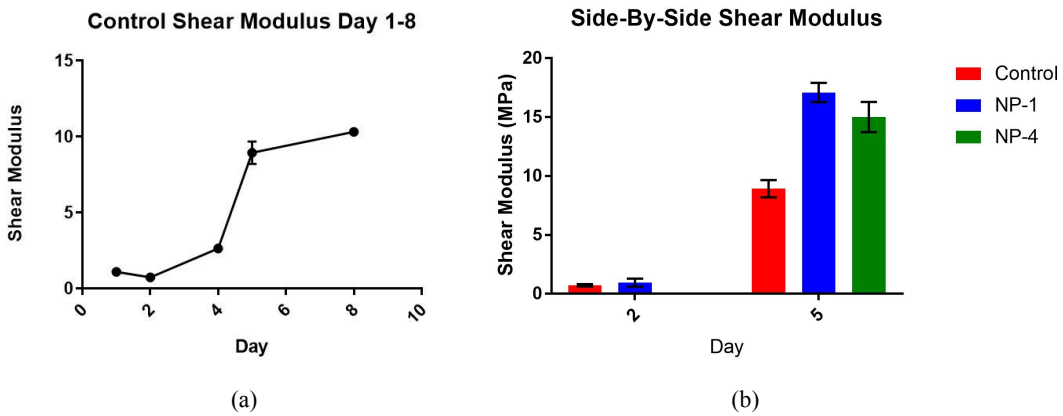


Fig. 2: Control, NP-1, NP-4 Shear Modulus Over Time
(a) graph of the control group's moduli shows the early day values of DPSC shear modulus on a hard PB surface, and (b) a side by side comparison with NP-1 and NP-4 groups. A larger modulus indicates a harder surface

In Figure 2(a), the average control shear modulus of 2.6374 at day 4 increases significantly to 8.9272 on day 5, then levels out to a modulus of 10.3035 at day 8. This confirms preliminary testing that suggested that DPSCs recognize their substrate near on day 4, spiking to day 5, as they adjust their cell mechanics accordingly to the underlying substrate mechanics. This was hypothesized to cause different effects of the NP's when added on day 1 versus 4, and Figure 2(b) suggests that the differences between NP-1 and NP-4 cells start from the original

uptake mechanisms. TiO_2 NPs seem to have entered the cells and affected the measurements of shear modulus, as both NP-1 and NP-4 showed a significantly higher modulus on day 5. Interestingly, while the difference in shear modulus between control and NP-1 one day after NP addition on day 2 is minimal, NP-4 shows significantly higher shear moduli than control one day after NP addition on day 5. This immediate jump in cell stiffness indicates a more substantial, rapid uptake of the TiO_2 NPs through a different uptake mechanism on day 2 versus day 5.

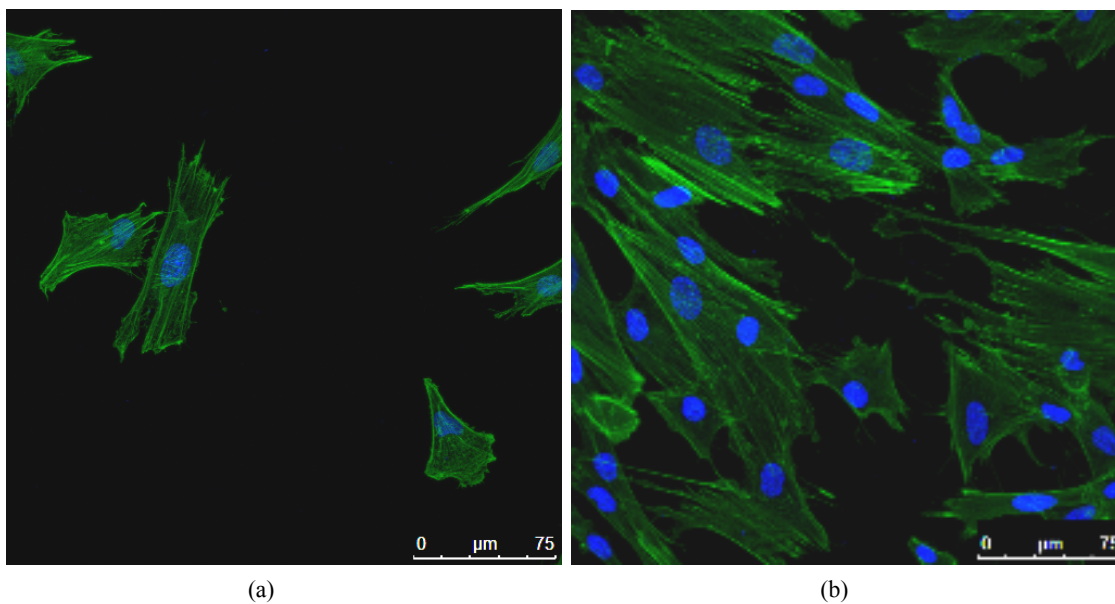


Fig. 3: Actin of Control DPSCs on Day 1 vs. 4
Confocal images of control DPSC cells on (a) day 1 and (b) day 4. Both images have brightness increased to view the actin (green stain) better.

Confocal imaging of actin scans further supports changing cell mechanics and nanoparticle uptake over time, as the mechanics of cells are related to the strength of actin fibers. As shown in Figure 3(a), actin filaments (shown in green in streaks) on day 1 are weaker and condensed, reflecting a soft and underdeveloped actin filament network. However, in Figure 3(b), day 4 DPSC actin filaments are well-stretched, thicker, and expansive, indicating a stronger, more rigid cytoskeletal structure.^{30,31} This growth of the actin filament network could allow for a change in nanoparticle uptake mechanisms, as actin networks are essential in

processes of endocytosis, or the internalization of particles in small vesicles.³² Large aggregates of much harder NP's taken up by actin-driven endocytosis could make the cell appear harder, and since the uptake process itself involves the utilization of actin fibers, specific regions of the cell itself would be harder, as actin fibers could locally increase to assist with the endocytosis. Both of these factors could explain the harder values of the cells with NPs on day 5 in Figure 2(b), and therefore, we hypothesize that endocytosis occurred to form vesicles of TiO₂ after day 4, while it could have been impossible at day 1, when the actin was weaker.

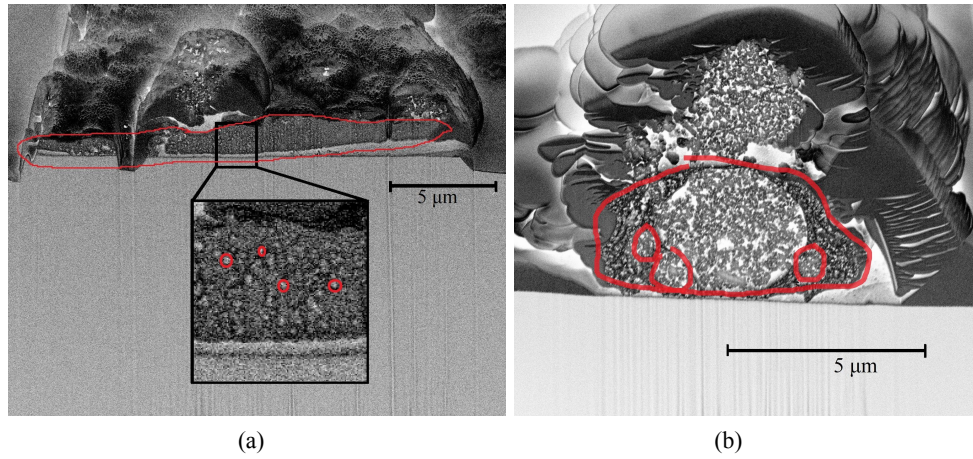


Fig. 4: FIB-SEM Cross Section Images
FIB-SEM images displaying NP uptake mechanisms with (a) SEM images of DPSC with particles added on day 1 (NP-1) from day 2 and (b) NP-4 on day 5 (both 24 hrs after adding particles). The red outlines the cells (middle grey colored) and some particles or groups of particles (white)

Cross sections of the DPSCs 1 day after NP addition by FIB-SEM imaging confirms that the particles were uptaken and further substantiates our hypothesis of substantial differences in NP uptake mechanisms from day 1 and day 4. Figure 4(a) illustrates cellular uptake on day 2, where NPs appear to be more distributive, scattered throughout the cell without organization. However, Figure 4(b) depicting day 5 shows NPs aggregated in clustered, vesicle-like structures, of which the cell in the figure has a large one in the center and smaller ones circled. This contrast suggests that there could be a difference in approach to NP uptake between the two timepoints.

While TiO_2 nanoparticles are able to permeate through the cell membrane in weaker cells without extracellular structure, more developed actin filament networks on later days of culturing might allow for cells to uptake particles through endocytosis in vesicles. Cells on days 1 and 4 thus possess different mechanical properties, which could affect the uptake mechanisms and might explain consequent effects of TiO_2 NPs on later differentiation and proliferation.

(III. B.) DPSC Proliferation

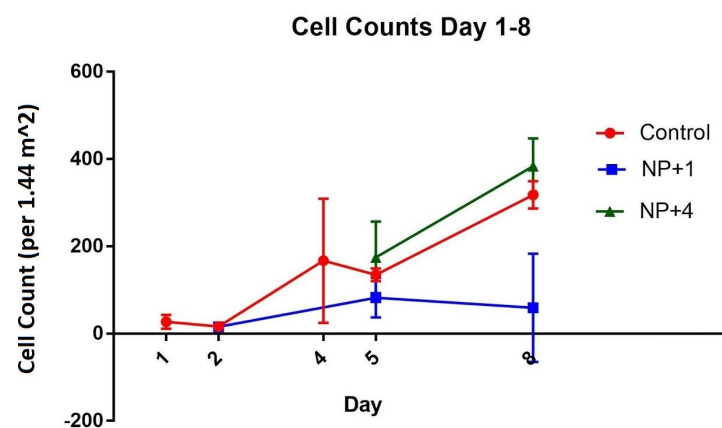


Fig. 5: DPSC Proliferation Over Days 1-8

Cell counts over early days were determined by the average in one confocal slide (1.2 mm on each side). The control data at day 4 has a lot of error and is probably too high, but a curve is still visualizable within the error range. The important comparisons also can be seen in days 5 and 8, where control and NP-4 have intersecting errors and NP-1 obviously performs worse

To investigate early cell proliferation, an indicator of cellular health, the stained nuclei in confocal images allowed for the counting of cells. The nuclei staining was used to allow the

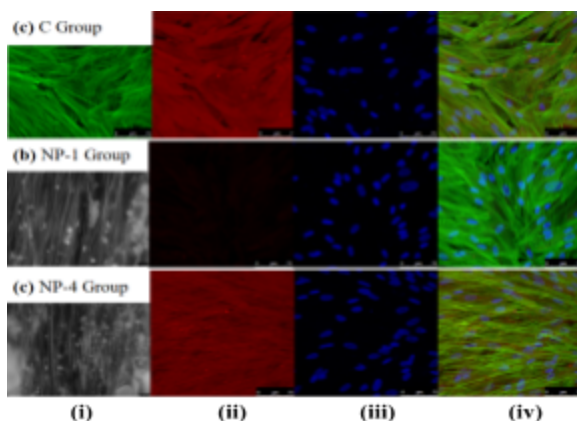


Fig. 6: Day 21 Confocal Microscopy Images
Images with (i) fluorescent (which sees TiO_2 and AF488), (ii) OCN stain, and (iii) DAPI nuclei stain filters. (iv) shows all of osteocalcin (red), nuclei (blue), and actin (green)

identification of cells for counting, which was done by viewing the confocal scans at a heightened contrast using the application ImageJ. Figure 5 depicts cell counts with DAPI-stained nuclei on full contrast performed on each day. While control shows increasing proliferation

between days 1 and 8, NP-1 is unable to grow significantly as proliferation stagnates. Our results challenge previous notions of TiO_2 as “safe” for cells, supporting recent studies indicating the cytotoxicity of TiO_2 NPs even at concentrations as low as 0.1 mg/mL. Figure 6(b)(iv) shows that NP-1 does recover and reach confluence by day 21, but DPSCs were harmed and the proliferation started off very slowly. On the other hand, by adding NPs on day 4, the short-term toxicity of TiO_2 NPs is limited, as control and NP-4 proliferate similarly from day 5 to 8. If the uptake mechanism hypothesis from earlier is applied to here, vesicles could protect the inside of a cell from direct contact with the nanoparticles, while the free-floating particles in NP-1 would have had a lot of time to damage internal components of cells. This study posits that the difference in short-term toxicity dependent on time of NP addition does exist, which could be accounted for by different uptake mechanisms.

(III. C.) DPSC Differentiation

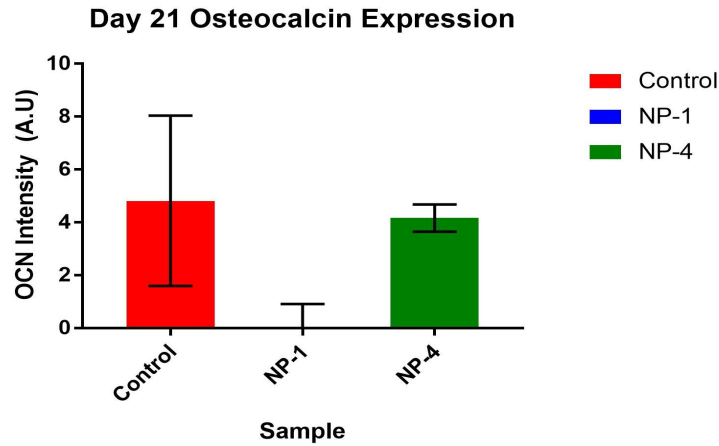
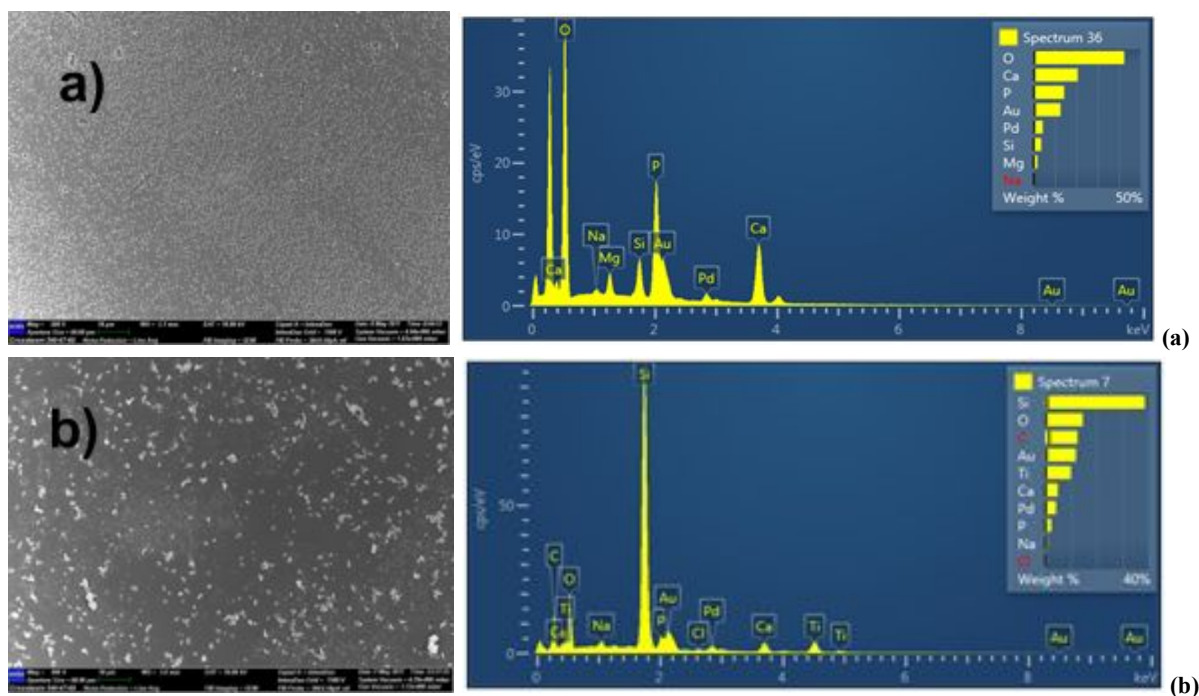


Fig 7: Day 21 Osteocalcin Expression
Cells were stained for OCN with anti-OCN primary and red fluorescent secondary. Relative intensities were then obtained by comparisons of confocal microscopy images of cells and the background.

To determine osteocalcin expression levels, we measured the relative intensity of OCN staining in confocal images on day 21, after osteocalcin has been able to be expressed. As shown in Figure 7, time of TiO_2 NP addition had large effects on later DPSC osteocalcin expression. DPSCs with addition on day 1 displayed entirely inhibited osteocalcin expression while DPSCs with addition on day 4 showed similar OCN expression to control when accounting for error. A single-tailed t-test reveals that NP-1 osteocalcin expression is suppressed when compared to control ($P = 0.07289$) while NP-4 and control show no significant difference ($P > 0.20$). NP-1 and NP-4 osteocalcin expression differences are much more significant ($P < 0.01$), likely due to the high error of the control OCN scans shown in Figure 7. Differences in OCN intensity (and similarity between control and NP-4) can be clearly seen in Figure 6(ii), demonstrating a difference in DPSC differentiation.



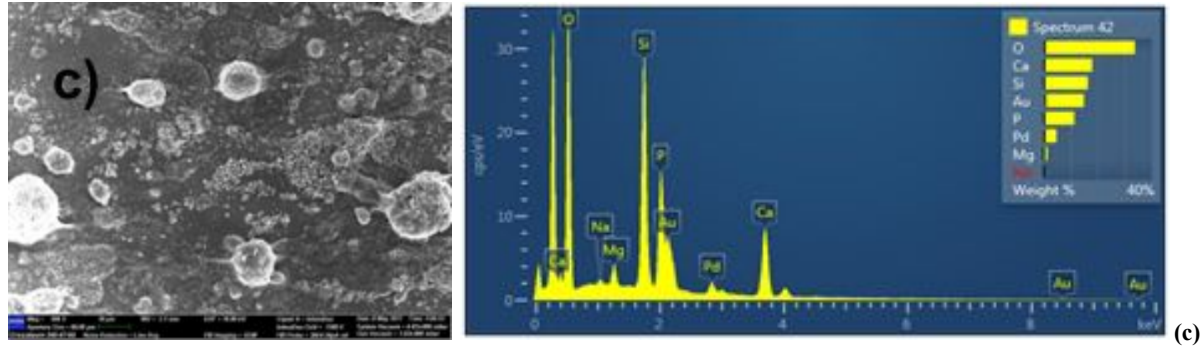


Fig. 8: SEM/EDX Biomineralization of DPSCs on Day 21

Day 21 SEM images after cells were detached from the substrate, leaving behind mineral deposits. Images were taken and EDX spectrums obtained for (a) the control, (b) NP-1, and (c) NP-4. The images are at 800x zoom and the spectrums are of regions with deposits.

Biomineralization (another indicator of differentiation) measurements further demonstrate the reduced harm of NPs in NP-4 compared to NP-1 on DPSC differentiation. Figure 8 depicts SEM/EDX scans comparing biomineralization of DPSCs with TiO_2 added on day 1 versus 4. Ca/P peaks in the ratio of 5:3 show the presence of hydroxyapatite ($\text{Ca}_5(\text{PO}_4)_3(\text{OH})$), a crystal compound in a bone matrix produced by osteoblasts that indicates osteoblast differentiation and formation.³³ As shown when comparing Figure 8(a) and (b), there is a much greater amount of deposits on the substrate for the control group, which has high Ca/P peaks with a ratio of 5:3. NP-1 does not have as much, and a lot of its deposits are TiO_2 (Ti and O). In Figure 8(c), NP-4 has much more biomineralization than NP-1, and it has high levels of Ca/P in the correct ratio, confirming the results of the OCN tests.

Based on osteocalcin intensity and biomineralization results, there is a substantial reduction in the harmful effects of TiO_2 NPs on DPSC differentiation when adding on day 4 rather than day 1, demonstrating that the timing of NP addition can prevent many potential drawbacks of utilizing TiO_2 NPs and NPs in general.

IV. Conclusion

Our results support the idea that TiO₂ NPs incur negative short-term proliferation effects and long-term loss of stem cell differentiability. These adverse effects discourage the uncontrolled usage of TiO₂ NPs in some sunscreen and toothpastes, which can also damage teeth and skin, preventing stem cells from being able to differentiate and heal wounds. However, by changing the time of particle addition in an *in vitro* environment, it is possible to reduce harm to DPSC viability. By being allowed to develop in their environment before being introduced to the NPs, NP-4 DPSCs did not suffer any of the negative effects our study found in NP-1 cells. This simple procedural change in NP addition allows safer assimilation of NPs into targeted cells without significantly affecting their differentiation and viability.

(IV. A.) Future Directions

While this study investigates the effects of TiO₂ NPs added at various times on DPSC differentiation and proliferation, further exploration is needed in multiple areas. Different substrates other than PB hard films can be tested in order to investigate the effects of the potential cellular response. Given more time, effects due to other NPs used in both dentistry and cell imaging such as SiO₂, ZnO, and Al₂O₃ added at different stages can be analyzed. Furthermore, this study shows a substantial difference in TiO₂ uptake into cells at different time points, as shown by SEM scans. More research is needed to examine the specific time-dependent mechanisms of NP uptake that could explain this discrepancy. Finally, this study only looks into mechanical properties as an explanation for differing time-dependent results. Further research into other factors affecting differentiation such as DPSC gene regulation is needed.

(IV. B.) Closing Remarks

In this experiment, DPSCs were observed to uptake TiO₂ NPs within 24 hours following exposure, and in the NP-1 group, which reflects normal toxicity tests, the TiO₂ did in fact affect the differentiation and proliferation of the DPSCs compared to the control with the outcome dependent on the time of exposure during the early stages of the differentiation process. For instance, both biomineralization and osteocalcin expression at day 21 were suppressed after the addition of TiO₂ NPs on day 1 before the DPSCs responded to the substrate mechanics. However, when the TiO₂ NPs were added 4 days after plating and after the cells sensed the substrate, biomineralization and osteocalcin expression were induced at levels that were the same as the control cell population, which signified that differentiation was unaffected. The early stage of NP uptake is different between DPSCs before and after they have fully responded to the substrate mechanics (observed by FIB-SEM). NPs are more dispersive inside the cells when added on day 1 and are more clustered when added at day 4, which we hypothesized to be a cause of the different results in proliferation and differentiation. We are also able to show that, in order to best prevent NP-induced developmental toxicity, TiO₂ NPs should be added to DPSCs after they have responded to a hard PB-coated silicon substrate on day 4. This simple approach allows for the use of nanotechnology in clinical medicine with a wide range of new diagnostic and therapeutic opportunities such as medical imaging, medical diagnosis,³⁵ drug delivery, and cancer management and treatment,³⁶ so long as the cells uptaking particles are allowed to adapt their mechanical properties in an *in vitro* environment. Ultimately, tests of the toxicity of NPs on human cells need to be redone for different timepoints, and if cells are truly healthier as well as viable, it opens the door to scientific and medicinal usage.

V. References

1. Mahla, R. S. (2016). Stem Cells Applications in Regenerative Medicine and Disease Therapeutics. *International Journal of Cell Biology*, 2016, 1–24. <https://doi.org/10.1155/2016/6940283>
2. NIH Stem Cell Information Home Page. (2017). Stem Cell Information. Retrieved 13 July 2017, from <https://stemcells.nih.gov/info/basics/1.htm>
3. Watt, F., & Driskell, R. (2009). The therapeutic potential of stem cells. *Philosophical Transactions Of The Royal Society B: Biological Sciences*, 365(1537), 155-163. <http://dx.doi.org/10.1098/rstb.2009.0149>
4. Chalissery, E. P., Nam, S. Y., Park, S. H., & Anil, S. (2017). Therapeutic potential of dental stem cells. *Journal of Tissue Engineering*, 8, 2041731417702531. <http://doi.org/10.1177/2041731417702531>
5. Yildirim, S. (2013). Dental Pulp Stem Cells. *SpringerBriefs in Stem Cells*. Springer New York. <https://doi.org/10.1007/978-1-4614-5687-2>
6. Hosoya, A., & Nakamura, H. (2015). Ability of stem and progenitor cells in the dental pulp to form hard tissue. *Japanese Dental Science Review*, 51(3), 75–83. <https://doi.org/10.1016/j.jdsr.2015.03.002>
7. Potdar, P. D., & Jethmalani, Y. D. (2015). Human dental pulp stem cells: Applications in future regenerative medicine. *World Journal of Stem Cells*, 7(5), 839–851. <http://doi.org/10.4252/wjsc.v7.i5.839>
8. Nguyen, P. K., Nag, D., & Wu, J. C. (2010). Methods to Assess Stem Cell Lineage, Fate and Function. *Advanced Drug Delivery Reviews*, 62(12), 1175–1186. <http://doi.org/10.1016/j.addr.2010.08.008>
9. Jomini, S., Clivot, H., Bauda, P., & Pagnout, C. (2015). Impact of manufactured TiO₂ nanoparticles on planktonic and sessile bacterial communities. *Environmental Pollution*, 202, 196–204. <https://doi.org/10.1016/j.envpol.2015.03.022>
10. Crosera, M., Prodi, A., Mauro, M., Pelin, M., Florio, C., Bellomo, F., ... Larese Filon, F. (2015). Titanium Dioxide Nanoparticle Penetration into the Skin and Effects on HaCaT Cells. *International Journal of Environmental Research and Public Health*, 12(8), 9282–9297. <http://doi.org/10.3390/ijerph120809282>
11. Mohamed Hamouda, I. (2012). Current perspectives of nanoparticles in medical and dental biomaterials. *Journal of Biomedical Research*, 26(3), 143–151. <http://doi.org/10.7555/JBR.26.20120027>
12. Shah, S. N. A., Shah, Z., Hussain, M., & Khan, M. (2017). Hazardous Effects of Titanium Dioxide Nanoparticles in Ecosystem. *Bioinorganic Chemistry and Applications*, 2017, 1–12. <https://doi.org/10.1155/2017/4101735>
13. Pan, Z., Lee, W., Slutsky, L., Clark, R. A. F., Pernodet, N., & Rafailovich, M. H. (2009). Adverse Effects of Titanium Dioxide Nanoparticles on Human Dermal Fibroblasts and How to Protect Cells. *Small*, 5(4), 511–520. <https://doi.org/10.1002/sml.200800798>
14. Cai, K., Hou, Y., Li, J., Chen, X., Hu, Y., Luo, Z., ... Lai, M. (2013). Effects of titanium nanoparticles on adhesion, migration, proliferation, and differentiation of

- mesenchymal stem cells. *International Journal of Nanomedicine*, 3619.
<https://doi.org/10.2147/ijn.s38992>
15. Tabari, K., Hosseinpour, S., Parashos, P., Kardouni Khozestani, P., & Rahimi, H. M. (2017). Cytotoxicity of Selected Nanoparticles on Human Dental Pulp Stem Cells . *Iranian Endodontic Journal*, 12(2), 137–142.
<http://doi.org/10.22037/iej.2017.28>
 16. Smijs, T. G., & Pavel, S. (2011). Titanium dioxide and zinc oxide nanoparticles in sunscreens: focus on their safety and effectiveness. *Nanotechnology, Science and Applications*, 4, 95–112. <http://doi.org/10.2147/NSA.S19419>
 17. Wang, Y., Xu, C., & Ow, H. (2013). Commercial Nanoparticles for Stem Cell Labeling and Tracking. *Theranostics*, 3(8), 544–560.
<http://doi.org/10.7150/thno.5634>
 18. Thurn, K. T., Brown, E., Wu, A., Vogt, S., Lai, B., Maser, J., ... Woloschak, G. E. (2007). Nanoparticles for Applications in Cellular Imaging. *Nanoscale Research Letters*, 2(9), 430–441. <http://doi.org/10.1007/s11671-007-9081-5>
 19. Parveen, S., Misra, R., & Sahoo, S. K. (2012). Nanoparticles: a boon to drug delivery, therapeutics, diagnostics and imaging. *Nanomedicine: Nanotechnology, Biology and Medicine*, 8(2), 147-166. <https://doi:10.1016/j.nano.2011.05.016>
 20. Shakeel, M., Jabeen, F., Shabbir, S., Asghar, M. S., Khan, M. S., & Chaudhry, A. S. (2015). Toxicity of Nano-Titanium Dioxide (TiO₂-NP) Through Various Routes of Exposure: a Review. *Biological Trace Element Research*, 172(1), 1–36.
<https://doi.org/10.1007/s12011-015-0550-x>
 21. Discher, D. E. (2005). Tissue Cells Feel and Respond to the Stiffness of Their Substrate. *Science*, 310(5751), 1139–1143.
<https://doi.org/10.1126/science.1116995>
 22. Tee, S.-Y., Bausch, A., & Janmey, P. A. (2009). The mechanical cell. *Current Biology : CB*, 19(17), R745–R748. <http://doi.org/10.1016/j.cub.2009.06.034>
 23. Lv, H., Li, L., Sun, M., Zhang, Y., Chen, L., Rong, Y., & Li, Y. (2015). Mechanism of regulation of stem cell differentiation by matrix stiffness. *Stem Cell Research & Therapy*, 6(1), 103. <http://doi.org/10.1186/s13287-015-0083-4>
 24. Jurukovski, Vladimir & Rafailovich, Miriam & Simon, Marcia & Bherwani, A & Chan, Chung-Chueng. (2014). Citation: Entangled Polymer Surface Confinement, an Alternative Method to Control Stem Cell Differentiation in the Absence of Chemical Mediators. *Annals of Materials Science & Engineering. Advances in Materials Science and Engineering*. 1. 3-2014.
 25. Cox, P. (2015). Chapter 9. Atomistic Modelling of Drug Delivery Systems. *Drug Design Strategies*, 210-231. <https://doi.org/10.1039/9781849733403-00210>
 26. Fischer, E. R., Hansen, B. T., Nair, V., Hoyt, F. H., & Dorward, D. W. (2012). Scanning Electron Microscopy. *Current Protocols in Microbiology, CHAPTER, Unit2B.2*. <http://doi.org/10.1002/9780471729259.mc02b02s25>
 27. Mori, G., Brunetti, G., Oranger, A., Carbone, C., Ballini, A., Muzio, L. L., ... Grano, M. (2011). Dental pulp stem cells: osteogenic differentiation and gene expression. *Annals of the New York Academy of Sciences*, 1237(1), 47–52.
<https://doi.org/10.1111/j.1749-6632.2011.06234.x>

28. Schneider, C. A., Rasband, W. S., & Eliceiri, K. W. (2012). NIH Image to ImageJ: 25 years of image analysis. *Nature Methods*, 9(7), 671–675.
<https://doi.org/10.1038/nmeth.2089>
29. Ji, Y., Li, B., Ge, S., Sokolov, J. C., & Rafailovich, M. H. (2006). Structure and Nanomechanical Characterization of Electrospun PS/Clay Nanocomposite Fibers. *Langmuir*, 22(3), 1321-1328. <https://doi.org/10.1021/la0525022>
30. Gong, J., Zhang, D., Tseng, Y., Li, B., Wirtz, D., & Schafer, B. W. (2013). Form-Finding Model Shows How Cytoskeleton Network Stiffness Is Realized. *PLoS ONE*, 8(10), e77417. <https://doi.org/10.1371/journal.pone.0077417>
31. Galletta BJ, Cooper JA. Actin and Endocytosis: Mechanisms and Phylogeny. *Current opinion in cell biology*. 2009;21(1):20-27.
<https://doi.org/10.1016/j.ceb.2009.01.006>
32. Yameen, B., Choi, W. I., Vilos, C., Swami, A., Shi, J., & Farokhzad, O. C. (2014). Insight into nanoparticle cellular uptake and intracellular targeting. *Journal of Controlled Release : Official Journal of the Controlled Release Society*, 190, 485–499. <http://doi.org/10.1016/j.jconrel.2014.06.038>
33. Clarke, B. (2008). Normal Bone Anatomy and Physiology. *Clinical Journal of the American Society of Nephrology*, 3(Supplement 3).
<http://doi.org/10.2215/cjn.04151206>
34. Zhang, F., Song, J., Zhang, H., Huang, E., Song, D., Tollemar, V., . . . Ji, P. (2016). Wnt and BMP signaling crosstalk in regulating dental stem cells: Implications in dental tissue engineering. *Genes & Diseases*, 3(4), 263-276.
<http://doi.org/10.1016/j.gendis.2016.09.004>
35. Yin, Z. F., Wu, L., Yang, H. G., & Su, Y. H. (2013). Recent progress in biomedical applications of titanium dioxide. *Physical Chemistry Chemical Physics*, 15(14), 4844. <http://doi.org/10.1039/c3cp43938k>
36. Chopra, D. (2011). Radiolabelled Nanoparticles for Diagnosis and Treatment of Cancer. *Radioisotopes - Applications in Bio-Medical Science*.
<http://doi.org/10.5772/20719>